HiFFUT - A New Class of Transducer

Update Report 1

Dr Andrew Feeney MEng(Hons) PhD CEng MIMechE

Research Fellow in the Centre for Industrial Ultrasonics

Department of Physics

University of Warwick

Coventry CV4 7AL, United Kingdom

a.feeney@warwick.ac.uk

March 24, 2017

Contents

List of Figures

General Overview

This report is intended to be an update of the HiFFUT research project up to March 2017. Included in this report are details of the studies into the electro-mechanical behaviour of a commercial flexural ultrasonic transducer, progress made in the design and fabrication of laser-welded flexural transducers, and developments in the design and fabrication of the required measurement vessels for the investigation of HiFFUT performance at high pressure and temperature levels.

The three principal sections included in this report are all detailed with a focus on how the knowledge will be used in the development of the demonstrator HiFFUTs. Commercial flexural transducers operate through a vibrating membrane, similar to the characteristic behaviour of a HiFFUT. Therefore, the electro-mechanical behaviour of a commercial flexural transducer is essential to understand. Furthermore, there is a long-standing problem in the consistency of fabrication of flexural transducers, a concern which directly translates to the manufacture of HiFFUTs. Therefore this research also has direct relevance to the project. The information contained in this report is supported with proposed details for the next steps of the research.

1. The electro-mechanical behaviour of flexural ultrasonic transducers

This section outlines research conducted with invaluable experimental contributions from two *M.Phys* dissertation students, Chris Wells and Mike Ginestier. It is known that the current range of flexural ultrasonic transducers possess high electro-mechanical coupling efficiency levels for ultrasound detection and generation in fluids. However, little is known in detail about the vibration response of such transducers, from the application of a driving signal, to the interaction between the driving voltage and the natural resonance of the transducer. This research has been collated and is intended to be published in *Applied Physics Letters*, with an expanded correspondence considered for a journal such as *Ultrasonics*. In this part of the research, a commercial ultrasonic transducer was used, the schematic for which is shown in Figure 1.1.

1.1 Analogue model of the transducer response

The purpose of the development of an analogue model is to support experimental investigation of the characteristics of the transducer in response to a range of driving conditions. There is a fundamental requirement for this research in order to ensure that these transducers are efficiently operated, and driven at their natural frequency, and is novel in terms of the supporting scientific literature.

The flexural transducer can be regarded as a system which operates in three distinct regimes. The first is a transient condition characterised by a ramp up to resonance and steady-state conditions, where the input amplitude and frequency of excitation approaches that of the natural frequency of the system, and dominates the response. The second is that particular steady-state

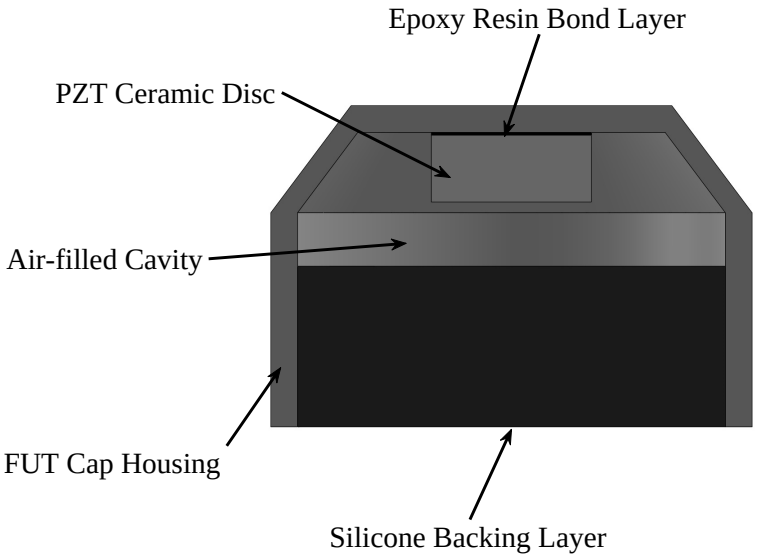

Figure 1.1: Schematic of the components of the commercial flexural ultrasonic transducer.

region in which the transducer is in operation at resonance and maximum output energy, and the third is a transient state where there is an absence of excitation forcing function, and the response of the system decays according to its natural frequency, until the response is zero.

The graphical schematic of the transducer is shown in Figure 1.2, where M represents the vibrating mass of the transducer, K the stiffness, and C the damping factors of the system. In this analysis, a lightly damped, or underdamped, oscillator is assumed. From this schematic, Equations 1.1 and 1.2 can be derived, which can be used to form the differential equation of motion, shown in Equation 1.3.

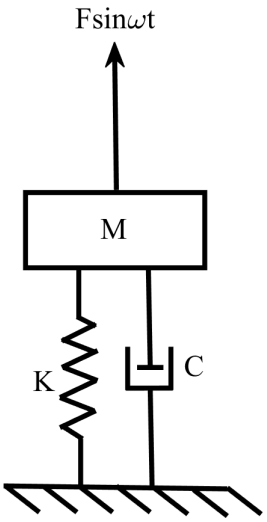

Figure 1.2: Analogue schematic of the transducer.

$$F_S = -Kx \tag{1.1}$$

$$F_D = C\dot{x} \tag{1.2}$$

$$M\ddot{x} = -C\dot{x} - Kx \tag{1.3}$$

Equation 1.3 can be rearranged for the case of free vibration according to Equation 1.4, where Equations 1.5 and 1.6 apply.

$$\ddot{x} = \frac{C}{M}\dot{x} + \frac{K}{M}x \tag{1.4}$$

$$\omega_n = \sqrt{\frac{K}{M}} \tag{1.5}$$

$$\zeta = \frac{C}{2M\omega_n} \tag{1.6}$$

A transient vibrating system, such as the vibrating flexural transducer, can be represented by Equation 1.7, assuming viscous damping in the decay regime.

$$x(t) = Xsin(\omega t - \phi) + Ye^{-\zeta\omega_n t}cos(\omega_D t + \theta) \tag{1.7}$$

In this equation, the X coefficient term is the steady-state response, and the Y coefficient term is the transient response. For **Stage 3**, the region in which there is a transient response of the transducer, the steady-state part of the expression in Equation 1.7 can be neglected, where it is assumed that the forced excitation does not act, and where the natural vibration, or ring-down, of the transducer dominates, decaying to zero. The expression for the free decaying response is shown in Equation 1.8.

$$x(t) = Ye^{-\zeta\omega_n t}cos(\omega_D t + \theta) \tag{1.8}$$

In this case, the amplitude constant, Y, and phase, θ, both depend on initial conditions. A lightly-damped structure is assumed, and so the damping term is less than the stiffness term. Therefore, ζ is less than 1.0. Assuming initial conditions for x and $\dot{x}$ equal to zero, it can be shown that the damped natural frequency of the transducer, ω_D, is given by Equation 1.9.

$$\omega_D = \omega_n\sqrt{1-\zeta^2} \tag{1.9}$$

For **Stage 2**, the region in which there is steady-state vibration, we can assume a linear response with vibration governed by Equation 1.10.

$$M\ddot{x} + C\dot{x} + Kx = Fsin\omega t \tag{1.10}$$

The particular solution for Equation 1.10 can be found through Equation 1.11.

$$x = Xsin(\omega t - \phi) \tag{1.11}$$

Equation 1.11 and its derivations can be used to substitute into Equation 1.10 to create expressions for the amplitude and phase angle can be produced, shown in Equations 1.12 and 1.13.

$$X = \frac{F}{K} \frac{1}{\sqrt{(2\zeta(\frac{\omega}{\omega_n}))^2 + (1 - (\frac{\omega}{\omega_n})^2)^2}} \tag{1.12}$$

$$\phi = tan^{-1} \frac{2\zeta\left(\frac{\omega}{\omega_n}\right)}{1 - (\frac{\omega}{\omega_n})^2} \tag{1.13}$$

Through the initial conditions of the vibration motion, which depend on the forced steady-state conditions of **Stage 2**, the expressions shown in **Stage 3** can account for a phase difference between steady-state and free decaying transducer responses. With both **Stage 2** and **Stage 3** defined, consideration can now be given to the generation of the forced excitation in the transducer, but in a transient state, since this occurs just before steady-state. This is the characteristic of **Stage 1**. It can be assumed that in this stage, forced oscillations towards resonance are produced in the transducer, from an initial rest condition.

In **Stage 1**, it is assumed that the vibration response is zero from rest, until a discrete time, after which steady-state is produced, the response of which is represented in **Stage 2**. The development of a mathematical equivalence, or analogue, for the transducer behaviour of **Stage 1** is centred on the fact that it is effectively an impulse signal used to drive the transducer to resonance. The approach for **Stage 1** is a convolution of the Heaviside step function with a sinusoidal forcing function of the form Xsinωt, with consideration of the natural transducer resonance in the analysis. The equation of motion and the excitation response of the flexural transducer in **Stage 1** is shown in Equation 1.14, with the initial conditions defined according to Equation set 1.15.

$$M\ddot{x} + C\dot{x} + Kx = Asin(\omega t).H(t_0 - t) \tag{1.14}$$

$$x = 0 \; and \; \dot{x} = 0 \; at \; t = 0 \tag{1.15}$$

In Equation 1.14, t_0 represents the time at which the excitation signal is switched off. For Equation set 1.15, the Heaviside function is zero for a time $t \leq 0$, but 1 prior to the beginning

of Stage 2, upon the ramp up to steady-state. Therefore, this derivation applies for the condition shown in Equation 1.16, where the full derivation is shown in Equations 1.17 to 1.18.

$$For\ 0 \leq t \leq t_0,\ H = 1. \tag{1.16}$$

$$x = A_+e^{\lambda_+ t} + A_-e^{\lambda_- t} + Bsin\omega t + Dcos\omega t, where\ (Bsin\omega t + Dcos\omega t) = \bar{B}sin(\omega t + \phi) \tag{1.17}$$

In Equation 1.17, the first two A terms, the homogeneous part of the equation, represent the natural resonance of the transducer. The second part of the equation defines the forced excitation, where $\bar{B} = \sqrt{B^2 + D^2}$, the amplitude response in **Stage 1**, and is derived to be expressed in terms of A. The expressions shown in this section for the amplitude and phase, Equations 1.18 and 1.19, are provided without the extensive derivation.

$$\bar{B} = \sqrt{\left(-\frac{(M\omega^2 - K)A}{\omega^2C^2 + (M\omega^2 - K)^2}\right)^2 + \left(-\frac{\omega CA(M\omega^2 - K)}{(M\omega^2 - K)(\omega^2C^2 + (M\omega^2 - K)^2)}\right)^2} \tag{1.18}$$

$$cos^2\phi = \frac{\left(-\frac{(M\omega^2-K)A}{\omega^2C^2+(M\omega^2-K)^2}\right)^2}{\left(-\frac{(M\omega^2-K)A}{\omega^2C^2+(M\omega^2-K)^2}\right)^2 + \left(-\frac{\omega CA(M\omega^2-K)}{(M\omega^2-K)(\omega^2C^2+(M\omega^2-K)^2)}\right)^2} \tag{1.19}$$

1.2 Experimental and numerical results

The experimental setup used to investigate the vibration response of the transducer is shown in Figure 1.3. A function generator is used to drive the transducer, the vibration of which is measured by a laser Doppler vibrometer. Both the drive signal and the response of the transducer are simultaneously monitored by an oscilloscope.

In each case, the drive signal consists of a 150-cycle sine-wave burst at an excitation voltage amplitude of 10V. A range of drive frequencies around resonance have been used to demonstrate the characteristics of the different vibration response stages, as detailed in Section 1.1.

For clarity, the resonance of the transducer can be determined by monitoring the amplitude response of the transducer with an oscilloscope for different drive frequencies.

The nominal resonance frequency of the transducer is 40kHz. Figure 1.4 shows the vibration response of the transducer for a drive frequency of 45kHz, slightly off-resonance, superimposed with the voltage signal.

Once the drive signal is switched off, the resonant ring-down transducer response has been identified, as shown in the inset of Figure 1.4. The transducer vibrates at resonance almost instantaneously, as long as the drive frequency is relatively close to the natural resonance frequency of the transducer. Figure 1.5 shows the experimentally-obtained amplitude-frequency relationship for different drive frequencies, where the resonance frequency (specifically at 41kHz) is clearly shown.

For drive frequencies close to resonance, the effective frequency smoothly converges towards the drive voltage frequency. However, for drive frequencies significantly far away from resonance, the effective frequency oscillates before converging on the drive frequency. It has been demonstrated that when the drive signal is stopped, the frequency of vibration approaches resonance almost immediately, with an exponential amplitude decay.

The analogue model developed in Section 1.1 can be used to compare with experimental data, and assess the suitability of the model for simulating the behaviour of the transducer. The response of the transducer at resonance is shown in Figure 1.7 for both experiment and the analogue model, and the response at different drive frequencies is shown in Figure 1.8. The results show that the proposed analogue model correlates well with the experimental response.

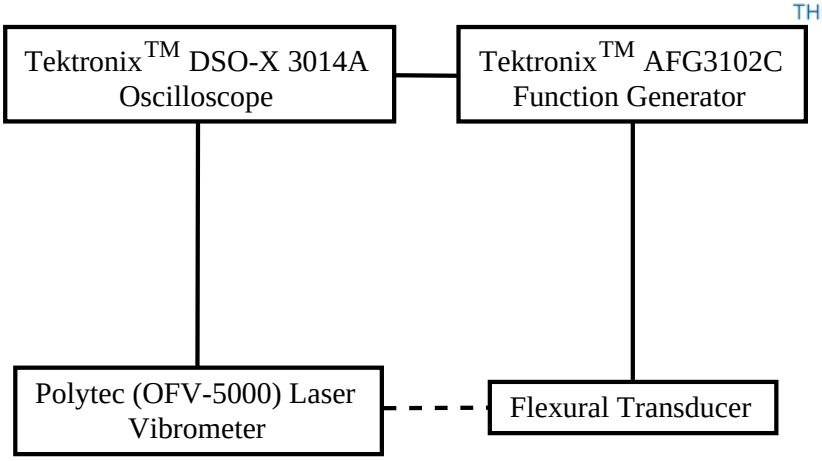

Figure 1.3: Experimental configuration used to analyse the vibration response of the flexural ultrasonic transducer.

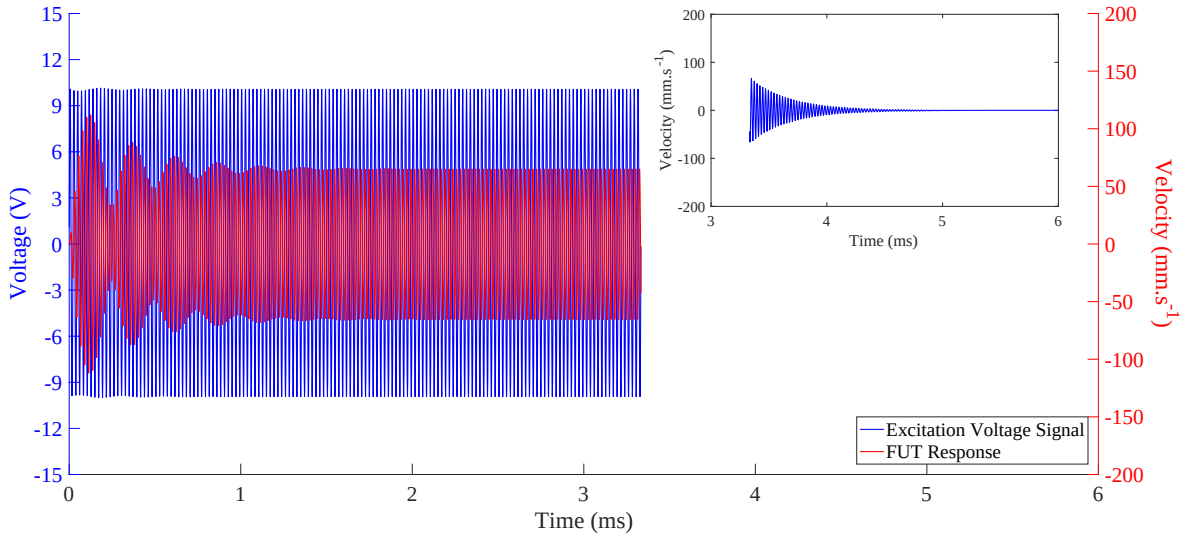

Figure 1.4: The measured excitation voltage signal superimposed with the velocity vibration response of the transducer, and (inset) the resonant ring-down response of the transducer upon the cessation of the drive signal. This measurement is shown for a 45kHz drive frequency, thus slightly off-resonance.

Using this information, the effective frequency response of the transducer at these drive frequencies has been demonstrated, as shown in Figure 1.6.

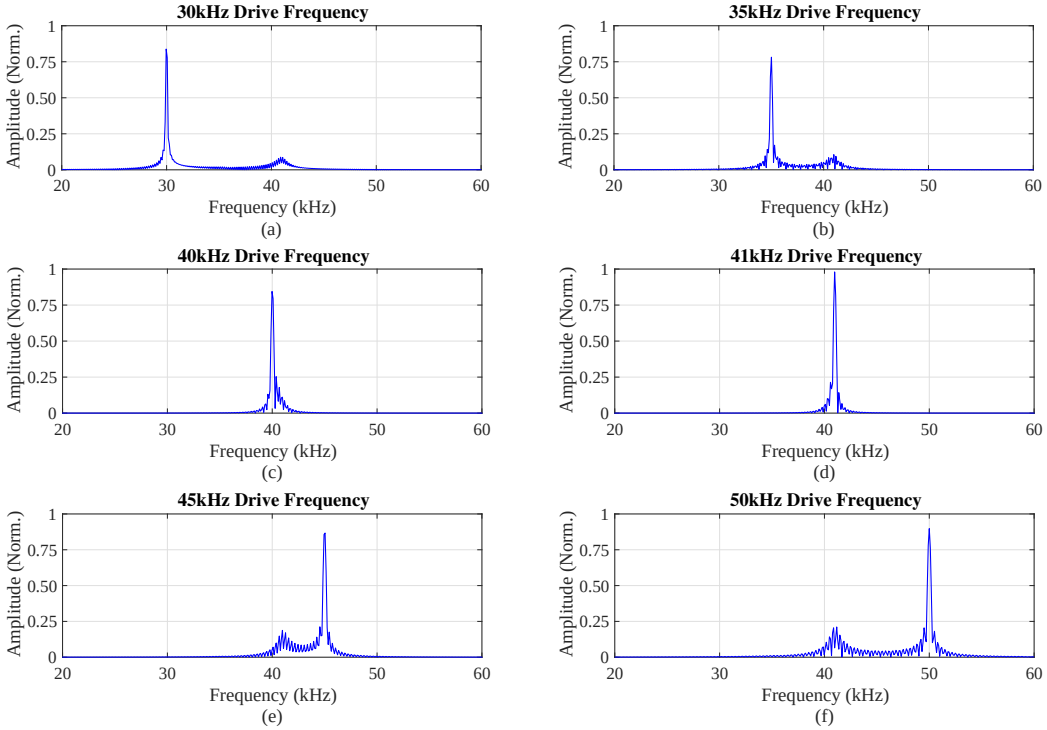

Figure 1.5: Normalised amplitude as a function of frequency, for a range of drive frequencies. The results are obtained from laser Doppler vibrometry measurements of the transducer on the centre of the vibrating membrane.

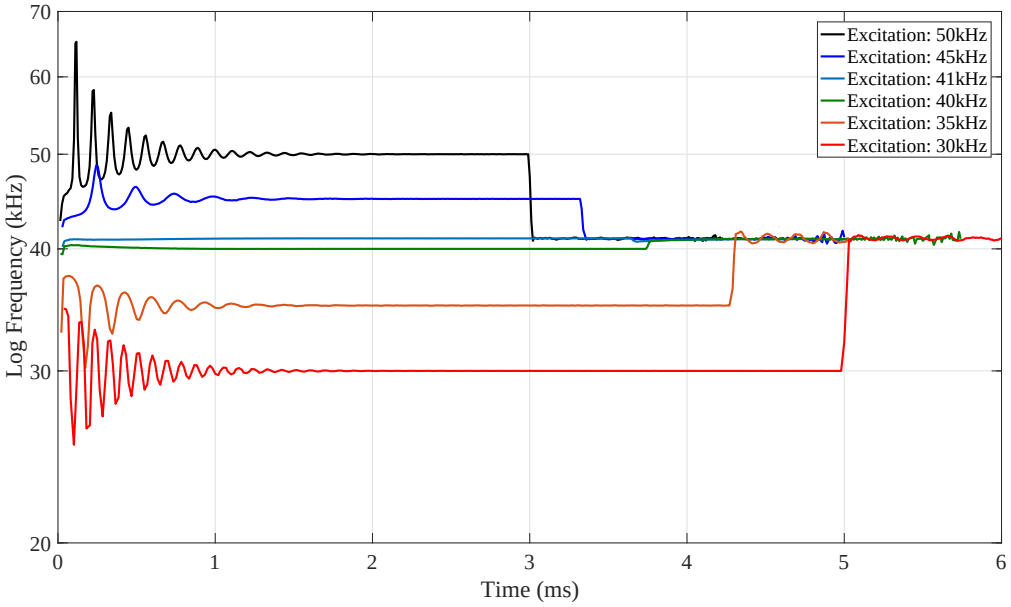

Figure 1.6: Effective frequency response for a range of drive frequencies.

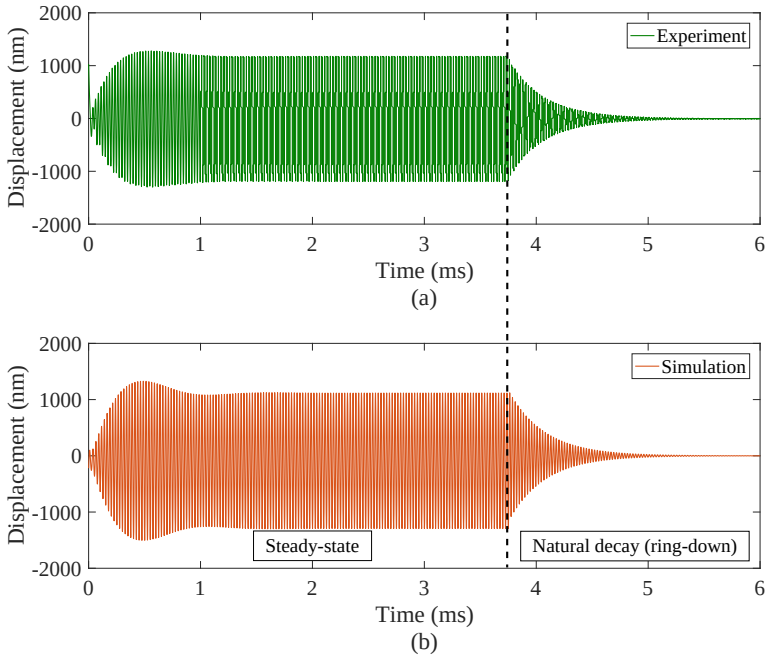

Figure 1.7: Response of the transducer at 40kHz, effective resonance, from (a) experimental and (b) analogue approaches.

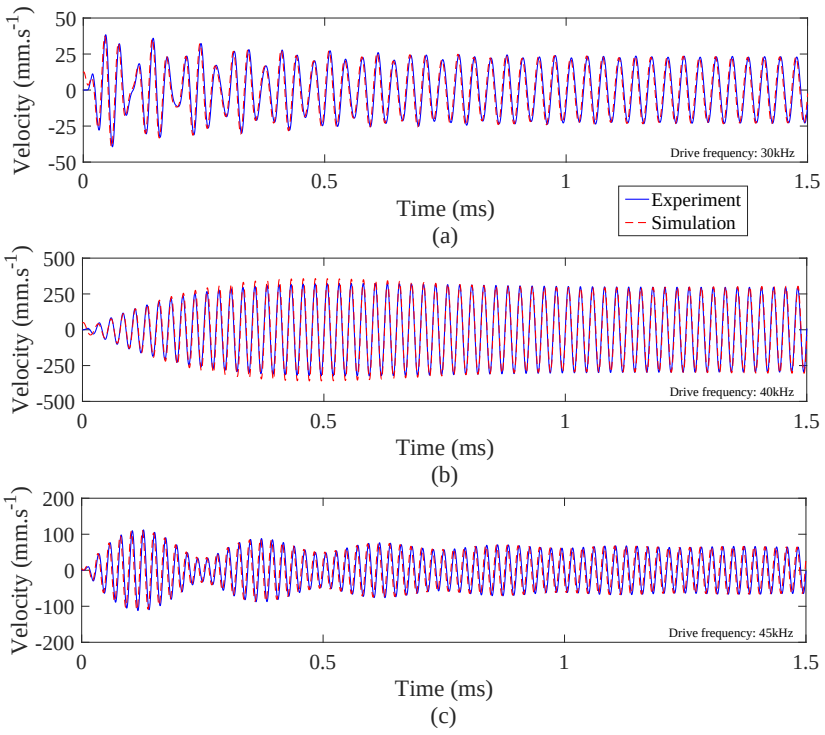

Figure 1.8: The *Stage 1* response of the transducer from experimental analysis, superimposed with fitted data, for three different drive frequencies.

1.3 Importance of this research to the project

The experimental measurements, complemented by the theoretical results from the analogue model, show three clear regions in the vibration response of a flexural transducer. There is an evident change in the measured ultrasound wave frequency based on the excitation condition of the transducer. This behaviour is essential to understand how flexural transducers work, and how they can be designed and operated most effectively for a range of applications. This directly impacts the design and operation of HiFFUTs, since they operate on a similar principle. One of the most important developments arising from this research is that the transducer resonance frequency can be measured very quickly and easily just by using an oscilloscope and function generator, so not requiring expensive equipment such as impedance/gain phase analysers.

2. Laser welding for the fabrication of HiFFUTs

This research proposes an alternative method of flexural transducer fabrication, which can be applied to the production of HiFFUTs. A major contribution to the inconsistencies between individual fabricated flexural transducers is from the bonding process. Current bond deposition and curing techniques cause differences between each transducer, particularly in the bond layer. The improvements to the transducer fabrication process can be assessed using two key experiments. The first is the analysis of the effect of the pre-loading process during the bond layer cure on the performance of the transducer. This can be performed using electrical response measurements, for example through acquisition of admittance loops using an Agilent 4294A impedance gain/phase analyser. The second is to observe the response of the transducer using laser Doppler vibrometry, comparing the measured mode shapes with those of FEA simulations, and the response of flexural transducers fabricated using conventional methods.

One way in which this problem can be addressed is through an adapted method of bond layer curing. It is proposed that the bonding agent is cured in a bespoke rig, as shown in the computer aided design (CAD) model in Figure 2.1, where the piezoelectric ceramic is bonded directly to a flat membrane. The advantage of this method is that the quantity of deposited bond material, the applied bonding pressure, and the uniformity of this applied pressure can all be more easily controlled.

The membrane can be placed in the centre of the lower square plate, where the deposition of bond material is performed. The piezoceramic disc is then positioned on top, and the top square plate of the rig is fixed in place. After this, a torque wrench can be used to load the rig to the desired curing pressure. Applying torque in small increments will be necessary to ensure a uniform pressure distribution, and to avoid fracture of the piezoceramic disc.

However, for this method to be practical, a technique of efficiently joining metal components

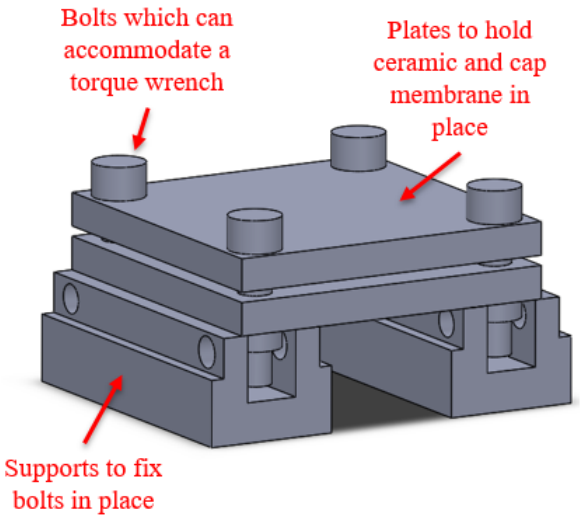

Figure 2.1: The bond curing rig design to improve the fabrication process for flexural transducers, and hence HiFFUTs.

together is required. This is proposed through the use of laser welding, where the membrane section of the metal cap with the piezoceramic disc bonded to it could be laser welded to a metal tube, forming the transducer cap side-wall. The laser welding of titanium is possible, but although the laser welding of titanium is the principal focus for this research, it is also possible to bond dissimilar metals.

First, a flexural transducer was modelled using PZFlex®, where titanium was defined as the cap material, and Bismuth Titanate (Ferroperm PZ46) was specified as the driver piezoelectric ceramic in the configuration, with properties sourced as available [1]. In the model, the BiT ceramic was defined as a 0.50mm thick disc with a diameter of 5.0mm. The resonance frequency of the (0,0) mode was designed to be above 50kHz. It is intended that the laser welding process is applied to the fabrication of a cap through the welding of a disc of metal with a lip, which will fit together with a separate component of titanium tubing, as shown in Figure 2.2.

The titanium sheet and tubing must therefore be sourced externally, and will be limited to standard sizes. The titanium supplier *Advent Research Materials* was chosen as the source of the raw titanium sheet material [2], and the tubing has been sourced from *William Gregor Ltd* [3]. The chosen tubing material based on the FEA data is ($13.70mm\ OD\ x\ 2.24mm\ WT$),

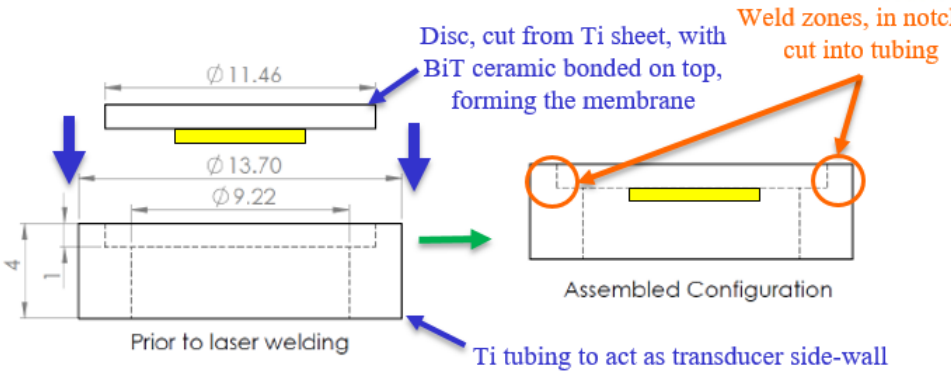

Figure 2.2: Schematic of the laser welding approach used in the fabrication of the BiT flexural transducer, where all dimensions are specified in millimetres.

made from Grade 2 titanium. The *WT* has to be wide enough in order to accommodate a small groove for laser welding to the membrane. The sheet material is 1.0mm-thick 99.6+% purity, temper-annealed titanium from *Advent Research Materials*, which must be machined into the appropriate disc shape. The results of the numerical simulations are shown in Figure 2.3, where the cap specification comprises an overall cap diameter, including side-wall thickness, of 13.70mm, a side-wall thickness of 2.24mm, and a side-wall length of 4.00mm. The resonance frequency of the (0,0) mode was calculated to be 74488Hz based on these dimensions, as shown in the frequency spectrum of Figure 2.3(a).

The performance of a BiT-based LWFT will be compared with LWFTs fabricated using PZT-5H (PZ29). Also, aero-glue will be used as a first step prior to the use of laser welding, to assess the performance of a transducer assembled from different constituent cap parts. The performance of the LWFT at high temperatures can be investigated, by using a high-temperature bonding agent, such as Epo-Tek 353ND. Epo-Tek 353ND can be used at a temperature of 250°C (continuous) or 350°C (intermittent). According to *Physik Instrumente (PI) GmbH & Co.*, a bonding pressure of around 5-7bar should be applied in the curing of Epo-Tek 353ND epoxy resin. The general process adopted in the development of laser-welded flexural transducers is shown below.

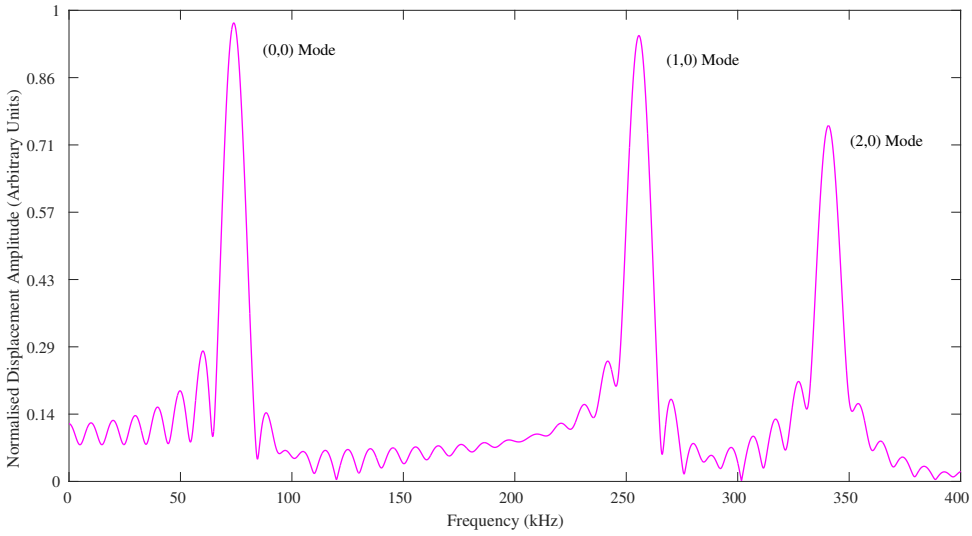

(a)

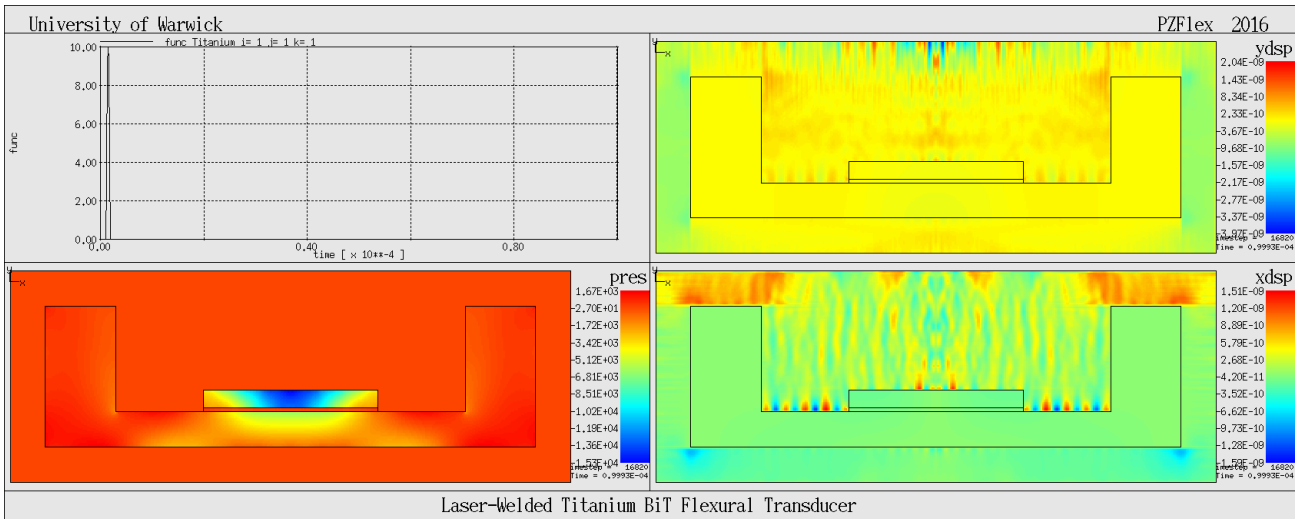

(b)

Figure 2.3: FEA simulation output produced in the design of the LWFT, showing (a) the resonance frequency response, and (b) an example radiation pattern for a half-cycle input signal at 600kHz.

1. Finite element modelling using PZFlex®, including optimisation of cap geometry to maximise the amplitude output of the (0,0) mode. As shown, the resonance frequency of the (0,0) mode is tuned to a high frequency, approximately 75kHz.

2. Measurement of the transducer response with electrical impedance analysis, where the impedance-frequency and phase-frequency responses as a function of temperature can be determined. This will be performed up to approximately 300℃.

3. Laser Doppler vibrometry at a suitably high temperature, such as 100℃ if possible.

3. Measurement Vessels for Pressure and Temperature

3.1 Pressure vessel design and fabrication

A pressure vessel has been designed in CAD, shown in Figure 3.1. This design was completed in order to be manufactured by *Gilwood (Fabricators) Company Ltd.*, with whom negotiations for fabrication are in progress. The design provides capacity for both gas and liquid at high pressure, around 200bar, and high temperature, up to 300°C, should either be required. The tests at high pressure will be conducted separately to those at high temperature, where the use of furnaces will be necessary. Therefore, the pressurisation system should incorporate suitable data acquisition capability. Any pressure and temperature sensors which are used will need to be integrated with the vessel architecture.

Regarding the general pressure vessel dimensions, the length of the vessel has been designed to be 300mm, which does not account for the thickness of the removable panels, and the outer diameter of the vessel has been specified as 100mm. The vessel should not be so large to require an inordinate amount of manual pressurisation, but should also be not too small such that the performance of the HiFFUTs cannot be easily analysed.

The pressure vessel incorporates a removable plate fixture at each end, so that multiple transducers can be set up inside. These removable panels include sealing or high-pressure glands which will permit cabling access, which is essential in order to drive the transducers, and for linking to measurement equipment. For example, temperature measurement may be necessary, and for this a standard RTD sensor will suffice, which can be placed directly in the internal pressure vessel chamber, with cabling through the glands in the removable plates.

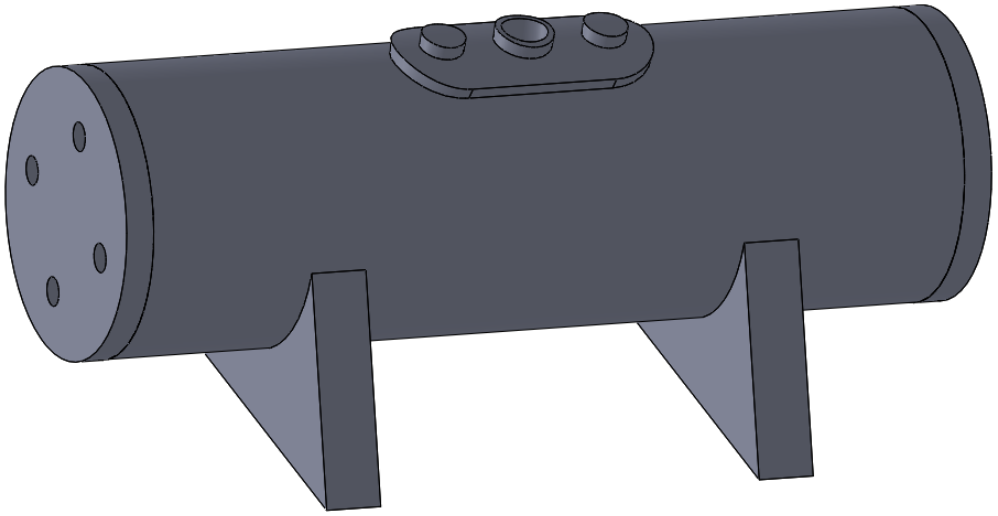

Figure 3.1: The final pressure vessel design, the schematic for which was delivered to Gilwood (Fabricators) Company Ltd.

An RTD such as Pt100 would be suitable for this investigation, and a material such as PFA Teflon^{TM} can be used to coat the RTD sensor for protection at high pressure levels. The vessel itself would simulate that of a pipe used in flow measurement, so it can be manufactured as a thin-wall pipe or cylinder. The main body of the vessel will include a valve panel, comprising a bleed-off valve, pressure-release valve, and a pressurisation port for connection to a pump system. The pump system chosen for this design is the MK4 Hill Pump, Unit 4128-005 [4]. This pump can operate to 4000psi (275.79bar), and possesses a hose with 1/8" BSP connection, which can be readily interfaced with the vessel.

Pressurisation with air is relatively simple using the MK4 Hill Pump. However, for the pressurisation of liquids such as water or oil, a flanged section has been specified in a flange layer in the vicinity of the pressure valves on the main body of the vessel. The purpose of this is to integrate a rubber-like layer which can be pressurised using the pump to generate a pressure in the vessel containing liquid, where the liquids are treated as incompressible fluids.

The design of the pressure vessel incorporates pressure sealing glands, sourced from *Thermal Detection Limited*. Specifically, they are *Multiple element sealing glands*, with supplier code

MHC2-020-A2-V, and have a process thread of 1/4"NPT, and are sealing 2x 0.020" OD elements with a Viton sealant. These sealing glands are designed to withstand the experimental 200bar pressure limit, and can accommodate multiple measurement probes. In total, four of these sealing glands are incorporated into the pressure vessel design, two on each end of the vessel. A schematic of the sealing gland is shown in Figure 3.2.

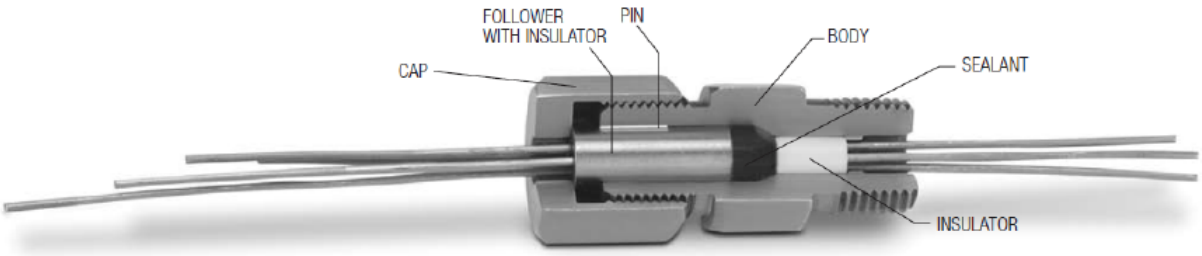

Figure 3.2: Schematic of the pressure sealing gland, four of which were sourced from *Thermal Detection Limited*.

3.2 Temperature vessel design and fabrication

A temperature vessel is required for the study of HiFFUT response at different temperature levels, and in a range of different media. Similar to the pressure vessel design described in Section 3.1, the temperature vessel can be fabricated in the form of a cylindrical tube. This cylindrical tube can be small enough to enable expedient heating of the HiFFUTs, with the capacity for the incorporation of external measurement probes and multiple transducers. The capability of the temperature control of the transducers in different media, such as gas, vacuum or air, is also essential.

The thermal equipment specialist *Carbolite® Gero* has been identified as a suitable supplier of equipment for temperature control, with capacity for customisation [5]. Specifically, the *Compact Horizontal Split Tube Furnace - EST / EZS* unit has been selected, shown in Figure 3.3.

Figure 3.3: The compact horizontal split tube furnace.

Key features of this temperature chamber are a 1200℃ operating temperature limit, fully-integrated temperature controller, and a range of heated lengths and diameters which can be accommodated within, giving flexibility to test subject design. In terms of customisation, over-temperature protection and a variety of digital controllers are among the additional features available for the equipment. Furthermore, specification of the modified atmosphere can be made at the time of purchase, so that the appropriate test conditions can be defined.

However, this unit may not be suitable for testing the HiFFUTs at high temperature in liquids. Therefore, it is proposed that a separate cylinder is designed for insertion into the tube cavity in the temperature chamber. This tube will be designed in a similar form to that of the pressure vessel, with space for measurement cable feed-through. Discussion with the temperature vessel manufacturer may be required at this stage, but the proposition is that a tube could be filled with liquid, part-way to account for expansion of the liquid as the temperature is raised, and the entire sealed tube with the HiFFUTs inside then placed in the temperature vessel for testing.

4. Summary and Next Steps

This research update report has intended to outline the progress made up to March 2017. As a broad summary, the electro-mechanical vibration behaviour of a commercial flexural ultrasonic transducer has been studied in depth, with results ready to be reported in the academic literature. These results have direct relevance to the design and operation of the HiFFUTs in this project. Also, most of the materials required for the laser-welding manufacture of flexural transducers have been acquired, with experimental research scheduled to commence in the upcoming second quarter of 2017. Finally, procurement of a pressure vessel should also be made in this time period. The immediate next steps for this research are outlined in the following list, with the updated Gantt chart shown in Figure 4.1.

1. Conduct laser welding to fabricate the Titanium caps.
2. Fabrication of a laser-welded flexural transducer with BiT piezoceramic driver, followed by a characterisation process comprising measurement of electrical properties of the transducer, including admittance loops to quantify the quality and coupling in the device. This method can be used to monitor transducer impedance, phase and resonance frequency as a function of temperature, to determine performance at high-temperature levels. Laser Doppler vibrometry at raised temperature, for example 100℃, to verify the mode shapes of the transducer. Radiation pattern measurement to quantify the output of the transducer.
3. Report on the influence of bonding pressure level on the performance of flexural transducers.
4. Finalise acquisition of the pressure vessel.
5. Design of candidate transducers for testing in a pressurised environment, around 200bar.

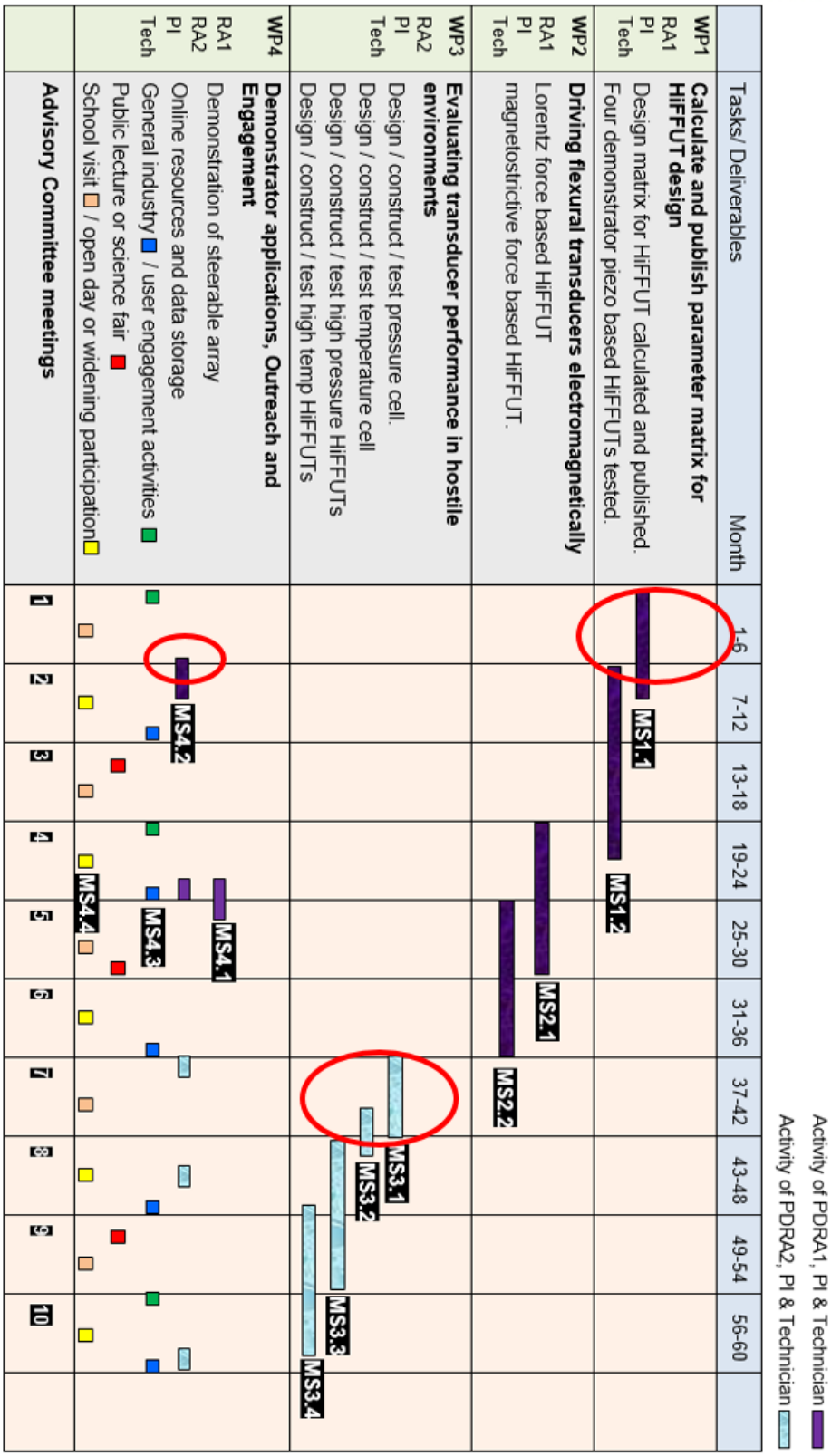

Figure 4.1: Gantt chart, indicating the areas in which the current research has addressed.

5. Acknowledgements

- Dr Andrew Tweedie, Pzflex Limited, for assistance with PZFlex® modelling.
- Mr Kevin Chan, Pzflex Limited, for assistance with PZFlex® modelling.
- Dr Susan Burrows, University of Warwick, for advice on BiT ceramic fabrication.
- Dr Lei Kang, University of Warwick, for advice on modelling and experimental testing.
- Dr Sam Hill, University of Warwick, for advice on modelling.
- Prof George Rowlands, University of Warwick, for assistance with analytical modelling.

References

[1] http://piezomat.org/materials/292.

[2] www.advent-rm.com.

[3] www.williamgregor.co.uk.

[4] www.airriflepump.com.

[5] www.carbolite-gero.com/products/tube-furnace-range/split-tube-furnaces/compact-tube-furnace.